

# Energy Recovery Soft Switching Improved Efficiency Half Bridge Inverter for Electronic Ballast Applications

A. Yazdanpanah Goharrizi

**Abstract**—An improved topology of a voltage-fed quasi-resonant soft switching  $LC_rC_{dc}$  series-parallel half bridge inverter with a constant-frequency for electronic ballast applications is proposed in this paper. This new topology introduces a low-cost solution to reduce switching losses and circuit rating to achieve high-efficiency ballast. Switching losses effect on ballast efficiency is discussed through experimental point of view. In this discussion, an improved topology in which accomplishes soft switching operation over a wide power regulation range is proposed. The proposed structure uses reverse recovery diode to provide better operation for the ballast system. A symmetrical pulse wide modulation (PWM) control scheme is implemented to regulate a wide range of out-put power. Simulation results are kindly verified with the experimental measurements obtained by ballast-lamp laboratory prototype. Different load conditions are provided in order to clarify the performance of the proposed converter.

**Keywords**—Electronic ballast, Pulse wide modulation (PWM) Reverse recovery diode, Soft switching.

## I. INTRODUCTION

UTILIZATION of voltage-fed quasi-resonant half-bridge inverters as AC sources is popular in a variety of applications including electronic ballasts [1-8]. These electronic ballasts help to improve lumen maintenance, eliminate flicker, lamp power control, light color and increase lifetime, thereby realizing high efficiency lamp power control.

In order to obtain compact electronic ballast, the operating frequency must be raised. However, at high frequency, soft commutation techniques are recommended to maintain high efficiency [2]. More studies are done to refine the circuit structure, in order to improve the ballast performances and reduce the circuit losses [3, 4 and 5]. Hence, the study presented in this paper proposes a novel improved topology of a voltage-fed quasi-resonant soft switching  $LC_rC_{dc}$  series-parallel inverter. This new topology introduces not only a low-cost solution to reduce switching losses but also an energy recovery feature to reduce energy consumption of ballast circuit. This advantages help system controller to regulate output power smoothly. To this end, a soft switching, high

efficiency, comparative low energy consumption and more controllable ballast is provided in this proposal.

In order to clarify the unique features of the new topology, different loads with different wattage and resistivity are utilized. In different load condition overall efficiency of the ballast are measured. Switching losses effect on ballast efficiency is discussed through experimental point of view. Simulation results are obtained by PSCAD/EMTDC software [8]. Experimental results not only verify simulation results but also describe both the operating principle and feasible feature of the new topology.

## II. THE PROPOSED INVERTER FOR ELECTRONIC BALLAST APPLICATION

Voltage-fed quasi-resonant  $LC_rC_{dc}$  PWM soft switching inverter with a constant-frequency for electronic ballast applications is depicted in Fig. 1. This topology which can decrease turn-off losses of  $S1$  and  $S2$  with lossless snubber capacitor  $C_s$  and can reduce recovery loss of  $Q_1$  by substituting a reverse blocking high frequency power switch is supplied by a DC-link voltage of 310 V.

The capacitor  $C_s$  is a high frequency film capacitor for realizing ZVS on the basis of quasi resonance. In order to reduce the rating voltage of the  $Q_2$  and as a result, achieving low cost inverter an auxiliary lossless high frequency diode

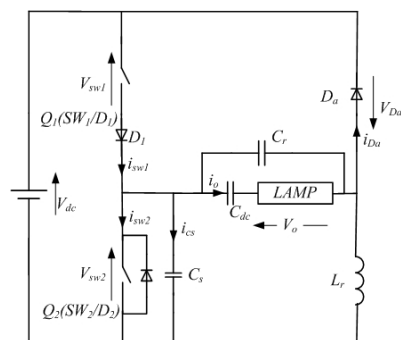


Fig. 1 The proposed improved half bridge inverter.

$D_a$  is utilized to the circuit. Consequently, an improved topology is obtained.

## III. EQUIVALENT RESISTANCE OF FLUORESCENT LAMP

The electronic ballast circuit operation can be developed in

A. Yazdanpanah Goharrizi is with Electrical Engineering Department , Islamic Azad University, Karaj Branch Karaj, Tehran, Tehran, Iran, ( e-mail: yazdanpanah\_tabu@yahoo.com and ar.yazdan@gmail.com ).

two distinct parts, firstly: ignition process, and secondly dimming operation. In the ignition process, the lamp is considered as an open circuit. Thus, during this operational stage, the series-resonant current through the ignition capacitor heats the two filaments and the voltage across the ignition capacitor ignites the lamp. On the other hand, during the dimming operation, the lamp is admitted as a variable resistance. In literature, several different models have been proposed to describe the behaviour of this equivalent resistance [9]. The calculated and measured lamp resistance versus lamp power is shown in Fig.2. Practical measurements were obtained from a simple 20 W fluorescent lamp. The calculated lamp resistance, obtained from [9]. Measured lamp resistance and the calculated lamp resistance agree well with each other when the lamp power is more than half of the full power. However, when the lamp power is low, there is a discrepancy between these two sets of figures.

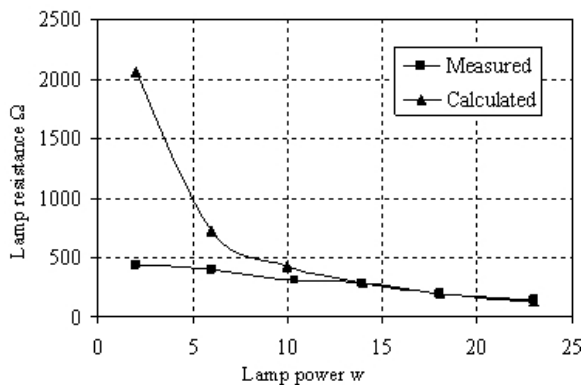


Fig. 2 Lamp equivalent resistance during dimming operation, at 24° C.

#### IV. SWITCHING OPERATION MODE

The step by step equivalent circuits of each mode are depicted in Fig. 3. Switches and diodes on-off states constitute each operation mode. Each operation mode is explained according to their circuit operation modes which are shown in Fig. 3. The value of circuit parameters and signal used for the simulation analysis are shown in table 1.

Mode 1 [ $t_0-t_1$ ] ( $S1$  is ON):  $S1$  is in the on state. In this mode the DC-LINK voltage of  $V_{dc}$  lets the resonant circuit to accumulate energy by supplying power through  $S1$  so resonant current through the lamp increases gradually. The inverter out-put power is controlled by the duration of this mode.

Mode 2 [ $t_1-t_2$ ] ( $C_s$  is discharged): When  $S1$  is turned off at  $t = t_1$ , the resonant current flowing through  $S1$  begins flowing for a short period through the snubber capacitor  $C_s$ .

TABLE 1  
CIRCUIT PARAMETERS OF THE PROPOSAL  $LC_rC_{dc}$  PWM SOFT SWITCHING HALF BRIDGE INVERTER

Term	Symbol	Value
AC power supply	$V_{in}$	110 V, 50 Hz
Input filter inductor	$L_{f1} \& L_{f2}$	2mH
Input filter capacitor	$C_{f1} \& C_{f2}$	100 nf
DC-LINK capacitor	$C$	22 $\mu$ f
Switching frequency	$f_s$	20kHz
Lossless snubber capacitor	$C_s$	12nf
Resonant capacitor	$C_r$	22nf
DC blocking capacitor	$C_{dc}$	1 $\mu$ f
Resonant inductor	$L_r$	2.2mH

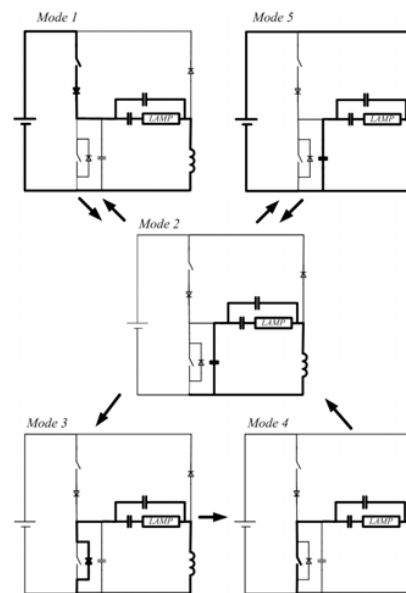


Fig. 3 Equivalent circuits in each switching operation mode.

In this process, a small amount of switching turn-off loss occurs when  $S1$  is turned off while retaining some values in voltage and current. As  $S1$  is turned off,  $C_s$  starts to discharge, and  $V_{S2}$  decays from  $V_{dc}$  to zero gradually. At the same time,  $V_{S1}$  rises from zero to  $V_{dc}$  gradually. Eventually, the anti-parallel diode  $D2$  becomes on-state when the charging of  $C_s$  is finished. By conducting  $D2$  this mode convert into mode 3.

Mode 3 [ $t_2-t_3$ ] ( $D2$  is ON): As the anti-parallel diode  $D2$  starts to conduct, the voltage of  $S2$  will reach zero. In this mode, the gate pulse voltage is applied to  $S2$ . While current of diode  $D2$  reaches zero the switch  $S2$  is turned on under ZVZCS conditions.

Mode 4 [ $t_3-t_4$ ] ( $S2$  is ON): Due to load resonance, the current freely resonates and flows in an inverse direction

through  $S2$  which is already turned on. Here, the resonant capacitor,  $C_r$ , serves as a voltage source. The lamp current flows in the loop of  $S2$ ,  $C_{dc}$ ,  $R_{lamp}$  and  $L_r$ .

Mode 2 [ $t_4$ - $t_5$ ] ( $C_s$  is charged): When  $S2$  is turned off at  $t = t_4$ , the resonant current flowing through  $S2$  starts to divert through the snubber capacitance  $C_s$ . In this process, a few amount of switching losses occurs at the turn-off transition. The resonant mode will continue until the voltage of inductor reaches to the DC-LINK voltage  $V_{dc}$ . From this time the auxiliary diode  $Da$  starts to conduct and this mode changes into mode 5.

Mode 5 [ $t_5$ - $t_6$ ] ( $Da$  is ON): The auxiliary diode  $Da$  acts as a reverse recovery diode. In this mode, the stored energy of the resonant circuit is converted to DC-LINK voltage  $V_{dc}$  through diode  $Da$ . This diode does not have to be fast because it conducts inductive current. The turn-on and turn-off losses of diode  $Da$  are almost zero because the turn-on and turn-off transition occurs under zero voltage condition. Consequently, the auxiliary diode does not impose additional losses to the inverter. This mode is regarded as non resonance mode. The equivalent circuit of this mode is shown in Fig. 4. The diode current is approximated by linear waveform in order to simplify both the calculation and discussion. Therefore in calculation of power and energy recovery just the peak current of diode  $Da$  is considered. This peak value can be easily calculated from the initial current and voltage values of this mode. The voltage drop across  $Da$  during on state is negligible.

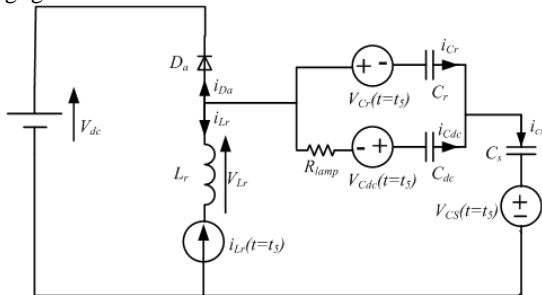


Fig. 4 Equivalent circuit of mode 5.

The initial diode current  $i_{Da}(t = t_5)$  can be calculated as follows.

$$i_{Da}(t = t_5) = i_{Cs}(t = t_5) - i_{Lr}(t = t_5) \quad (1)$$

where  $i_{Lr}(t = t_5)$  and  $i_{Cs}(t = t_5)$  are the initial values of inductor ( $L_r$ ) and capacitor ( $C_s$ ) currents respectively. The value of  $i_{Cs}(t = t_5)$  obtains from.

$$i_{Cs}(t = t_5) = i_{Cdc}(t = t_5) \frac{1}{(C_r / C_s) + 1} \quad (2)$$

Where  $i_{Cdc}(t = t_5)$  is the initial value of capacitor ( $C_{dc}$ ) current. The KVL in lobe  $L_r$ ,  $C_r$  and  $C_s$ , yields to

$$V_{Lr}(t = t_5) = V_{Cr}(t = t_5) + V_{Cs}(t = t_5) \quad (3)$$

Where  $V_{Lr}(t = t_5) \approx V_{dc}$  and  $V_{Cs}(t = t_5) = V_{dc}$  so the (3) yields to  $V_{Cr}(t = t_5) \approx 0$  therefore initial capacitor  $C_{dc}$  current is obtain from

$$i_{Cdc}(t = t_5) = \frac{V_{Cdc}(t = t_5)}{R_{lamp}}$$

By defining the values of  $i_{Lr}(t = t_5)$  and  $i_{Cdc}(t = t_5)$  from pervious modes the value of  $i_{Da}(t = t_5)$  can obtain from (1).

Equation (4) simplifies the calculation of the power that is sent from inductor to the DC-LINK voltage  $V_{dc}$  through diode  $Da$ .

$$P_r = \frac{1}{2} V_{dc} i_{Da}(t = t_5) f_s (t_6 - t_5) \quad (4)$$

Where  $P_r$  and  $f_r$  are the recovery power and switching frequency respectively.  $(t_6 - t_5)$  is the duration of mode 5. Therefore, the reverse recovery energy,  $W_r$  could approximately define as

$$W_r = \frac{1}{2} V_{dc} i_{Da}(t = t_5) (t_6 - t_5) \quad (5)$$

The average in-put power consumption is reduced by recovering this energy. As diode  $Da$  current falls to zero it goes to turn-off state and this mode convert into mode 2.

Mode 2: [ $t_6$ - $t_7$ ] ( $C_s$  is discharged) In this mode  $C_s$  conducts to discharge the excessive energy and its voltage fell into the DC-LINK voltage  $V_{dc}$ . At  $t_7$ , the switch  $S1$  turns on and this mode returns to mode 1.

#### V. MEASURED SWITCHING OPERATION WAVEFORMS OF THE PROPOSED INVERTER

The observed waveforms of the switches, auxiliary diode  $Da$ , snubber capacitor  $C_s$  and the lamp at the duty cycle  $D = 0.46$  are shown in Fig. 5. A 20W florescent lamp is used in laboratory prototype to measure these waveforms. It verifies the waveforms obtained by the simulations which will be show in Full Manuscript. Hence, the validated of the simulation becomes evident. In particular, switches  $S1$  and  $S2$  are found to turn-on under ZVS and ZCS operation.

Additionally, as can be seen from figures because of lossless snubber capacitor  $C_r$ , the switch,  $S2$  is free from EMI but the switch,  $S1$  has some oscillations. It should be noted that the diode peak current waveform is a little less than the one obtained from simulation. This is due to the assumption was made in the diode and resonant inductor that they are ideal. Moreover, unwanted oscillatory waveforms are observed in most of figures, which are not found in the simulation analysis. As can be seen in the Fig. 5(c), these phenomena occur at the turn-on times of the auxiliary diode. They probably come from the charges accumulated at the junctions of the diode, which may flow in an oscillatory way, owing to the capacitances of the diode and the stray inductances in the circuit etc. the oscillations at the instantaneous turn off and turn of the switches are inevitable, effected the current waveform of the snubber capacitor.

Additionally, as can be seen from figures because of lossless snubber capacitor  $C_r$ , the switch,  $S2$  is free from EMI but the switch,  $S1$  has some oscillations. It should be noted that the diode peak current waveform is a little less than the

one obtained from simulation. This is due to the assumption was made in the diode and resonant inductor that they are ideal. Moreover, unwanted oscillatory waveforms are observed in most of figures, which are not found in the simulation analysis. As can be seen in the Fig. 5(c), these phenomena occur at the turn-on times of the auxiliary diode. They probably come from the charges accumulated at the junctions of the diode, which may flow in an oscillatory way, owing to the capacitances of the diode and the stray inductances in the circuit etc. the oscillations at the instantaneous turn off and turn of the switches are inevitable, effected the current waveform of the snubber capacitor.

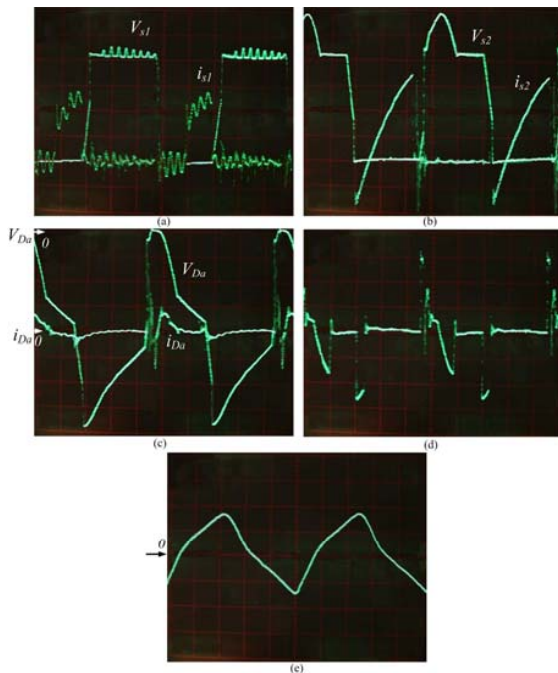


Fig. 5 Observed waveforms versus duty cycle. (a) Voltage and current of switch  $S1$  (50 V/div, 0.2 A/div,  $10\mu s/div$ ). (b) Voltage and current of switch  $S2$  (50 V/div, 0.2 A/div,  $10\mu s/div$ ). (c) Voltage and current of auxiliary diode (50 V/div, 0.1 A/div,  $10\mu s/div$ ). (d) Current of snubber capacitor (0.2 A/div,  $10\mu s/div$ ). (e) Lamp voltage (50 V/div,  $10\mu s/div$ ).

#### VI. ANALYSIS OF THE CONVERTER PERFORMANCE UNDER DIFFERENT LOAD CONDITION

In this section the converter behavior from output and input waveforms point of view is analyzed. In order to provide a good analysis, different fluorescent lamps with different length and wattage are used. A brief description of the lamps is depicted in the table 2. This description originates from experimental point of view.

TABLE II  
LAMP PARAMETERS USED IN LABORATORY PROTOTYPE

fluorescent lamp	Length	Steady state resistance
40 W	1.2 m	352.60 $\Omega$
20 W	0.5 m	148.0 $\Omega$
15 W	0.35 m	82.750 $\Omega$

#### VII. COMPARATIVE STUDY

Fig. 6 shows the DC to AC power conversion efficiency of the conventional and proposed

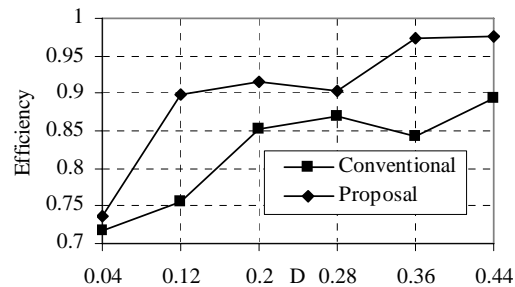


Fig. 6 DC-AC efficiency of conventional and proposal electronic ballasts against duty cycle  $D$ .

electronic ballast as a function of the duty cycle. These results are obtained from laboratory prototype which has got a 20 W lamp, mentioned in section 4, as its load. As can be seen, an extremely high efficiency of 99% is attained at  $D = 0.36$  while the rated out-put is supplied. Also, a fairly high efficiency of about 90% is obtained at  $D = 0.12$  when the minimum out-put power is feeding due to the soft switching of the switches. In addition, the soft-switching operation can be attained at a wide range of  $0.1 < D < 0.44$ .

#### VIII. CONCLUSION

In this paper a low switching losses  $LC_rC_{dc}$  series-parallel inverter using an auxiliary high frequency inverter has been presented. The inverter attains soft-switching operation and regulates its out-put power continuously over a wide range with the aid of a symmetrical PWM technique. Therefore, the electronic ballast provides high efficiency, low cost, small size and low energy consumption compared to the conventional electronic ballast. Examination of the experimental results confirm that wide dimming range and soft switching can be achieved over a wide duty cycle range in the proposed topology. The proposed converter offer great degree of flexibility in the variety load conditions which are provided with different lamp of wattage and resistance.

#### REFERENCES

- [1] Jesús Cardesín, José Marcos Alonso, Emilio López-Corominas, Antonio J. Calleja, Javier Ribas, Manuel Rico-Secades, and Jorge García, "Small-Signal Analysis of a Low-Cost Power Control for LCC Series-Parallel Inverters With Resonant Current Mode Control for HID Lamps," IEEE Trans. Power Electron., vol. 20, pp. 1205-1212, Sep. 2005.

- [2] [2] Sandra Johnson, and Regan Zane, "Custom Spectral Shaping for EMI Reduction in High-Frequency Inverters and Ballasts," *IEEE Trans. Power Electron.*, vol. 20, pp. 1499-1505, Nov. 2005.
- [3] [3] J. Marcos Alonso, Antonio J. Calleja, Javier Ribas, Emilio López Corominas, and Manuel Rico-Secades, "Analysis and Design of a Novel Single-Stage High-Power-Factor Electronic Ballast Based on Integrated Buck Half-Bridge Resonant Inverter," *IEEE Trans. Power Electron.*, vol. 19, no 2, pp.550-559, Mar. 2004.
- [4] B. Wang; X. Xiao," Application of multi-mode control strategy in the automotive HID headlight systems, " *WCICA 2008 7th World Congress*, June 2008, pp. 8064 - 8068
- [5] Z. Jian-dong, S. Zhi-yi; W. Zi-shang; W. Zhong-hua; "Research on integrated technology of intelligent control and electrical ballast for solar low pressure sodium lamp," *IPEMC '09. IEEE 6th International May 2009*, pp. 1259-1262
- [6] K. H. Liu and Y. L. Lin, "Current waveform distortion in power factor correction circuits employing discontinuous-mode boost converters," in *Proc. IEEE PESC'89*, 1989, pp. 825-829.
- [7] Stephen T. S. Lee, Henry Shu-Hung Chung, and S. Y. (Ron) Hui, "Use of Saturable Inductor to Improve the Dimming Characteristics of Frequency-Controlled Dimmable Electronic Ballasts," *IEEE Trans. power electron.*, vol 19, pp. 1653-1660, Nov. 2004.
- [8] Manitoba HVDC Research Center, PSCAD/EMTDC: Electromagnetic transients program including dc systems, 1994.
- [9] F. T. Wakabayashi and C. A. Canesin, "A new model for tubular fluorescent lamps operated at high frequencies for dimmable applications," in *Proc. IEEE ISIE'03*, 2003.